

PalArch's Journal of Archaeology of Egypt / Egyptology

Stability Assessment of Droop Controlled Hybrid Islanded Multiple Subgrids during Power Sharing

¹ Harikrishna Muda, ²K. Naga Sujatha, ³SMIEEE, T. Mahesh, ⁴C. Bhargava

¹ Post Doctoral Associate, National Institute of Advanced Studies, IISc Campus, Bangalore

² Professor, JNTUH College of Engineering Hyderabad

³ Assistant Professor, Institute of Aeronautical Engineering, Hyderabad

⁴ Associate Professor, Sreenidhi Institute of Science and Technology, Hyderabad

Harikrishna Muda, K. Naga Sujatha, SMIEEE, T. Mahesh, C. Bhargava: Stability Assessment of Droop Controlled Hybrid Islanded Multiple Subgrids during Power Sharing-- Palarch's Journal Of Archaeology Of Egypt/Egyptology 17(9). ISSN 1567-214x

Keywords: Distributed Energy Resources (DERs), hybrid ac/dc microgrids, bidirectional power flow, Autonomous control, small signal stability analysis, droop method

ABSTRACT

This paper investigates the issue of the small-signal stability of Hybrid Islanded Multiple Subgrids (HIMSs) formed by AC Subgrid (ACS) and DC Subgrid (DCS) clusters interconnected through a group of interlinking converters (ICs). Distributed energy resources (DERs) are controlled using a droop-based method. This control mechanism of ICs indirectly adjusts the load power of ACS and DCS using droop gains. Further, power sharing among the ACS and DCS is achieved accordingly. A linearized system model and analysis of autonomous operation of HISs is developed. Further, the eigen value based sensitivity analysis for HISs is presented to assess the impact of change in load condition, IC location, line resistance and dc droop gain value conditions. Furthermore, the sensitivity of system poles to variation in IC droop gain constant is identified. The set of eigen value trajectory plots are included to confirm the movement of system poles. It is found the pole move further inside the negative real plane for increasing power flow from DCS to ACS. Extensive scenarios are presented to demonstrate the system stability under the HIS control strategy with respect to different droop gain constants.

1. Introduction

THE hybrid ac/dc multiple subgrids are evolving towards the integration of renewable based Distributed Energy Resources (DERs) for promoting an energy future [1]. A portion of one or multiple AC Subgrids (ACS) and DC Subgrid (DCS) can be operated in Hybrid Islanded Multiple Subgrid (HIMS) mode, in which the AC or DC DERs and loads are connected in the ACS or DCS respectively [2]. A parallel operation of bi-directional interlinking converters (ICs) is involved to transfer power among multiple ACS and DCSs. The islanded mode can provide power to AC or DC loads during a loss of grid is shown in Fig. 1. For the stable and economic operation of HIMS, the active and reactive powers are shared among the DERs simultaneously.

The non-communication based and communication based control concepts for power sharing in hybrid microgrids are mentioned in [3]. The control techniques based on droop characteristics are applied. Depending upon the voltage and frequency reference points, the real and reactive powers are adjusted, which are independent of communication [1]. In the case of islanded mode of operation, the voltage or frequency are negotiated if the loads are not enough to absorb the generated power. In [4], adaptive droop gain method based on virtual voltage and frequency frame is proposed, which effectively control the real and reactive power flows independently and improve the system stability performance. To preserve power sharing stability, a decentralized control scheme based adaptive transient droop function is presented in [5]. In [6] decentralized control strategy based on additional droop gain constant is proposed for power sharing in ac microgrids. However, the small inaccuracies in inverter frequency output could result in increased circulating currents and system instability during islanded multimicrogrids scenarios [35].

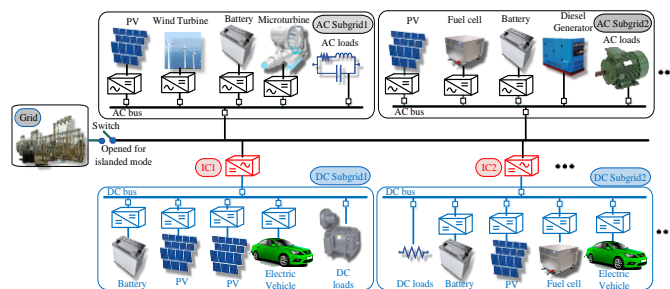


Fig. 1: Topology of the hybrid AC/DC multiple subgrids.

Focusing on the ICs, different operating modes of HIMS are discussed in [7]. A normalized bidirectional droop control based scheme is proposed for controlling ICs with the defined common per-unit range of the droop characteristics of ACS and DCSs [8][9]. The droop coefficient of IC unit is determined according to its KVA rating. In order to control the power transfer between the subgrids and achieve balanced power sharing of the system demands with minimum power losses, a new method correlating the requested load in the ACS and DCS is proposed in [10]. However, the load demand has to be measured accurately to manage the power exchange [11]. The stability

study based on state-space modeling approach and small-signal approach based on the linearization around an operating point and calculating the eigen values is proposed in [12]. It is shown that integral gain yields the system to stable region of operation as compared with proportional gain constant. Stability analysis indicated that the higher droop constants may shifts the dominate poles to the right hand leading to oscillatory response which compromise system stability [13], [14]. A stability margin is identified for the droop gains for each operating point in order to meet the desired damping. In order to enhance the stability, a phase compensation transfer function has been added to the unified power control loop in [15]. It is to be noted that the stability conditions for microgrids is limited to 3.3% from the nominal frequency, while deviation in voltage magnitude is limited to 5% from the nominal distribution level voltage [16].

The small-signal-based stability analysis has been reported in [17] to study the stability of the autonomous microgrid system. The stability margin is significantly affected by the loss of DERs in HIMSSs. Further, the presence of system poles in the stable region is also depends on droop gains, control parameters and system loading level. The impact of connecting ACSs and DCSs using ICs on stability is not considered. The factors such as the system-level dynamic interactions, power penetration, control schemes, droop coefficients, loads, line parameters etc. have been reported to affect the small-signal stability in [18]. An active virtual admittance compensation method is implemented in ICs to mitigate the interaction dynamics in hybrid microgrids networks.

A general structure of a cluster of interconnected ac and dc microgrids is shown in Fig. 2. It is to be noted that the two AC (or dc) microgrids are interconnected through AC/AC (or DC/DC) converters to provide bidirectional power flow on present generating and loading conditions of each microgrids. The active power and reactive power flowing through i^{th} IC is represented by P_i and Q_i respectively. In this paper we only considered the AC/DC subgrid interconnection scenario. Power sharing in ACS and DCS is controlled autonomously based on their traditional AC/DC droop control characteristics. All ICs are able to operate by means of a droop control system implemented as discussed in the next section.

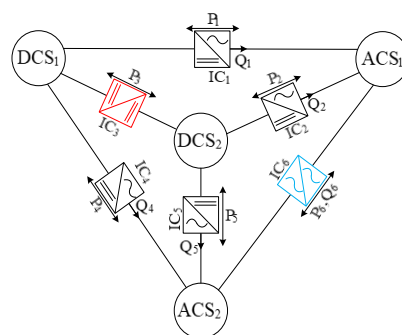


Fig. 2: Possible layout of different ac and dc microgrids interconnection with bidirectional power flow.

In this paper, the issue of the small-signal stability of HIMSs formed by ACS and DCS clusters interconnected through a group of ICs is considered. To establish the small signal model of hybrid microgrids, the state space average method is adopted. Sensitivity analysis results show that by transferring more power from ACS to DCS in comparison to DCS to ACS, the stability margin of the HIMS can be improved. With the addition of ACS and IC power capacities, the modified droop gain characteristics for the HIMS is presented.

2. System Under Study

Schematic diagram of a hybrid system which consisting of grid, ICs (3 in number), ACSs (2 in number) and DCSs (2 in number) is shown in Fig. 3. Each subgrid having sources, lines with distributed loads. The ICs are considered to provide bidirectional power among different type of subgrids. The subgrids can be operated in grid-connected mode as well as islanded mode by closing or opening switch, S as shown in Fig. 3. The DCS and ACS systems comprise the nominal voltage of 400 V and 220 V, 50 Hz respectively. The total maximum capacity of ac system is 20KVA with each subgrid capacity of 10KVA. Whereas, the each DCS has a maximum capacity of 10KW. There are local loads connected at each bus in subgrids. The sum of distributed loads in each subgrid is taken as 100% of its generation capacity. The dashed lines are used to mark the border of individual subgrids. The subgrid loads have been increased or decreased such that power is transferred by ICs.

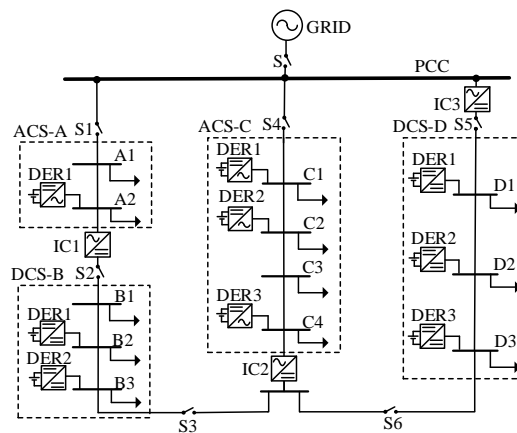


Fig. 3. Hybrid multimicrogrids system under study

In order to analyze the small signal stability behavior of different HIMSs, switches (S1 to S6) are deployed among subgrids. This model shown in Fig. 3 is adopted from [48]. Initially, subgrids A and B are studied in interconnected operating mode by operating the IC₁ and switch, S₂. Further, the electrical connection following subgrids A-B-C and B-C-D is considered as a possible HIMSs configuration with the bidirectional power flow among ACS and DCS. With these configurations, the corresponding HIMS small signal stability performance is evaluated for parallel operation of ICs. The ACS and DCS system parameters shown in Table 1 and Table 2 respectively. The DERs in each subgrid and ICs are equipped with conventional droop control strategies

to share the power among DC and AC loads. A detailed mathematical model of each control method is analyzed in this section.

Droop control for ACS

The AC DER consist of three-phase voltage source converter (VSC) fed from renewable energy or dispatachable sources. A DC source are used to emulate a source such as PV array, wind turbine or energy storage system. Fig. 3 depicts the detailed structure of a typical droop controlled DER in the ACS.

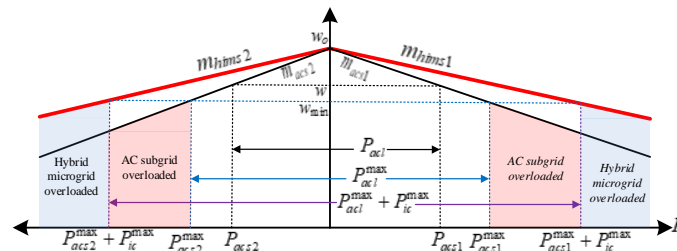


Fig. 4: The illustration of the droop lines of the two ACSs and HIMS with the loading conditions.

Droop control for ACS and DCS:

Usually, based on the local measurement of active and reactive power output at the DER terminal, the frequency and AC terminal voltage of the DER are regulated autonomously. Mathematically, the active power/frequency (P/f)-reactive power/voltage (Q/V) based droop controllers for the i^{th} DER can be expressed as

$$w_i = w_i^* - m_{aci} P_{aci} \tag{1}$$

$$E_i = E_i^* - n_{aci} Q_{aci} \tag{2}$$

where w_i^* and E_i^* are rated angular frequency and voltage amplitude respectively. P_i and Q_i are active and reactive power outputs respectively. m_i and n_i are active and reactive power droop gains, respectively. w_i and E_i are reference angular frequency and voltage amplitude of the DER respectively.

For the case of DERs in DCS, the coupling between DC terminal voltage and available power output is generally used and mathematically for i^{th} DER can be written as

$$V_i = V_i^* - m_{dci} P_{dci} \tag{3}$$

Where V_i^* and V_i are the rated and reference magnitude of the DC terminal voltage respectively. M_{dci} and P_{dci} are droop gain and active power output of the i^{th} DER respectively.

The power sharing between ACS and DCS is achieved based on the measurement of ac frequency and DC voltages of ACS and DCS. Further, using the droop characteristics shown in Fig. 4 the load capacity in each subgrid can be obtained indirectly. Which is the summation of the individual

loads. The equivalent maximum capacity of ACS (P_{acs}^{max}) can be obtained by summing all of the DER maximum capacity in ACS. While, the maximum capacity of DCS (P_{dcs}^{max}) is derived from the sum of all of the DER maximum capacity in the DCS.

Based on the ranges specified for the frequency of the i^{th} ACS, their active power droop gain (m_{acsi}) can be obtained written as

$$m_{acsi} = \frac{W_{max} - W_{min}}{P_{acsi}^{max}} \tag{4}$$

The slopes of the aggregated droop gain (m_{dcsi}) of i^{th} DCS can be acquired as

$$m_{dcsi} = \frac{V_{max} - V_{min}}{P_{dcsi}^{max}} \tag{5}$$

where V_{max} and V_{min} are the maximum and minimum allowed dc voltages of DCS respectively.

Droop control for ICs

Droop controllers for IC based on normalized values of ac frequency and the dc voltage were considered, and used to achieve flexible power flow among ACS and DCS. Since the ac frequency and dc voltage are independent physical quantities, their common range of pu values are calculated.

The droop control scheme implemented in the IC is shown in in Fig. 5. The r_f , l_f and c_f are the resistance, inductance and capacitance of filter, respectively. The DER and ICS are modelled as controllable voltage sources and, hence, fast switching dynamics of the converters are not considered in this paper. The IC voltage is v_{ic} , current is i_{ic} and the voltage at the terminal of DCS is v_{dc} . For the IC, the output voltage at the ACS terminal is v_o and the output current is i_o . A three-phase phase-locked loop (PLL) method is used to measure the operating frequency of IC and synchronization angle θ is used transform abc stationary frame to dq0 rotating frame. Details of the IC parameters can be found in the Appendix.

As shown in Fig. 5, the control of each individual IC consists of two parts, i.e., the normalization and current controller. The purpose of normalization is to bring the different droop variables used by two consolidated sources (ac frequency and dc terminal voltage) to a common per unit range. Further details can be found in [26] written by authors. Through normalization process, respective ac frequency and dc voltage equations for the i^{th} IC are frames as

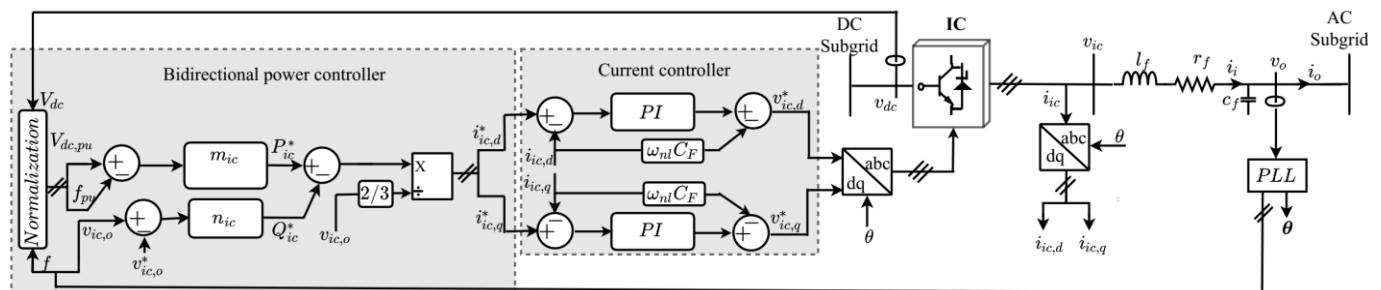


Fig. 5. Diagram of the droop control scheme for interlinking converter. (VSC in place of IC)

$$\widehat{w}_i = \frac{w_i - 0.5 \times (w_{\max} + w_{\min})}{0.5 \times (w_{\max} - w_{\min})} \tag{6}$$

$$\widehat{V}_i = \frac{V_i - 0.5 \times (V_{\max} + V_{\min})}{0.5 \times (V_{\max} - V_{\min})} \tag{7}$$

Where \widehat{w}_i and \widehat{V}_i are the normalized frequency and normalized DC voltage respectively. The current controller is based on traditional proportional integral (PI) controllers.

Similar to (4), the active power droop gain (m_{himsi}) for the i^{th} HIMS, can be rewritten as

$$m_{himsi} = \frac{W_{\max} - W_{\min}}{P_{acsi}^{\max} + P_{ic}^{\max}} \tag{4}$$

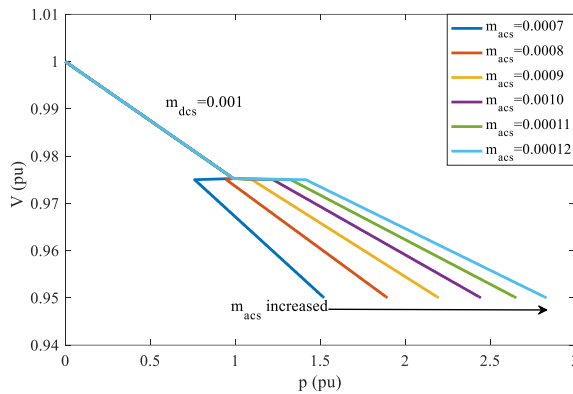


Fig. 6: combined droop curve for the DC subgrid

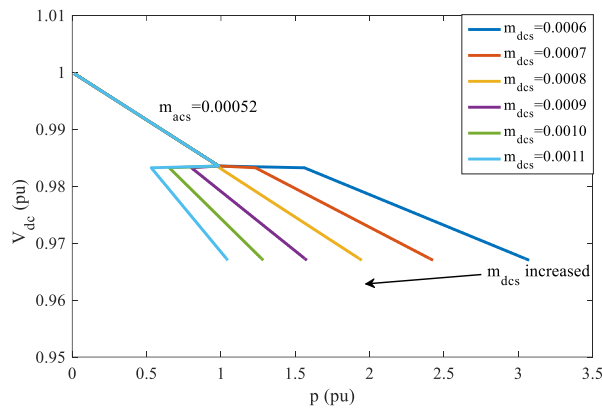


Fig. 7: combined droop curve for the AC subgrid

To investigate the impact of AC droop gain constant on the DC subgrid and impact of the DC droop gain constant on the AC subgrid, the droop gain characteristics for hybrid microgrid are depicted in Fig. 6 and Fig. 7. In Fig. 6. The m_{acs} increased from 0.0007 to 0.00012. The analysis is performed when the active power droop gain of dc sub grid is fixed at $m_{acs} = 0.001$. As it is observed, HIMS is more stable when the m_{acs} is increased. Moreover, the power generation capacity can be improved when the ac droop gain droop gain is increased and, accordingly, the stability margin of the system improves.

Similar analysis is performed by varying dc droop gain and fixing the ac droop in order to determine the impact of dc droop gain constant on the ac sub grid. It is observed that the stability margin can be improved when the dc droop gain constant is reduced which allows more generation capacity in the ac subgrid.

3. Small-Signal Modeling and Analysis

Small-signal analysis can provide a useful tool to analyze the control system and study the dynamic performance in power system [18]. The aforesaid equations can be linearized around an equilibrium point and the generalized state-space model of IC can be formulated as

$$\dot{\Delta x_{ic}}(t) = A_{ic} \Delta x_{ic}(t) + B_{ic} \Delta u_{ic}(t) \quad (22)$$

where $x_{ic} = [i_{ic,dq,j} \ v_{dc,j} \ P_{ic,ac,j} \ \phi_{ic,dq,j}]^T$ in which A_{ic} and B_{ic} are the state and input matrices given in [37].

The overall HMS system embeds individual small-signal model of different inverters combined with the small-signal model of ICs, ac and dc subgrids, network impedances and loads. The overall linearized model of HMS system developed in [37] is used, This can be given in the standard form of

$$\dot{\Delta x_{HMS}}(t) = A_{HMS} \Delta x_{HMS}(t) + B_{HMS} \Delta u_{HMS}(t) \quad (23)$$

The complete small signal model of the HMS derived in the form of (23) is used in the following sections. A linearized Jacobian matrix is therefore calculated around the nominal HMS operating point for system shown in Fig. 3. The derived Jacobian matrix is used as the basis for subsequent analysis.

4. Simulation Results

The system, shown in Fig. 3, is modeled in MATLAB/Simulink environment [42] to verify the power sharing analysis in the preceding sections.

Sensitivity Analysis

The sensitivity of the eigen values to change in system parameters is studied to further characterize the small-signal stability of the HMS and shown in Fig. 3. The system parameters used for the sensitivity analysis are the active power droop gains (m_{ac} , m_{dc} , m_{ic}), line impedances and loads. In the first step of analysis, the sensitivity of eigen values of the HMS is compared with individual ac and dc subgrids (ACS1 and DCS1). The connection among subgrids ACS1, DCS1 and ACS2 is considered as a possible HMS configuration. Further, two conditions, power flow direction from ac to dc subgrid and dc to ac subgrid are considered. The sensitivity of eigen values to change in power direction through ICs is studied.

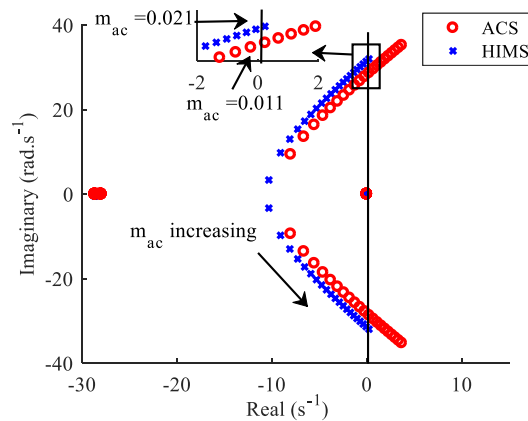


Fig. 8: Comparison of low frequency modes for variation of ac droop gain on ac subgrid and HMS: $2.5e-6$ pu (0.05% droop) $\leq m_{ac} \leq 0.021$ pu (4.2% droop).

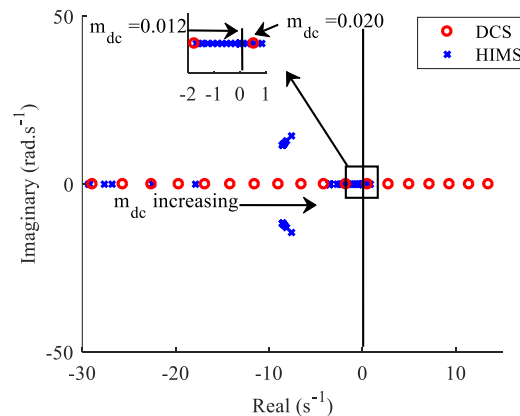


Fig. 9: Comparison of low frequency modes for variation of dc droop gain of dc subgrid and HMS: $2.5e-6$ pu (0.05% droop) $\leq m_{dc} \leq 0.021$ pu (4.2% droop).

1) Comparison of Impact of ac droop gain on ac subgrid and HMS

The eigen value analysis for two scenarios like ACS1 and HMS is considered. The trajectory of dominant low frequency eigen values are presented in Fig. 8. The variation of droop gain of ac subgrid is increased from $2.5e-6$ pu to 0.021 pu. It is observed that the HMS is stable for wide range of ac droop gain value in comparison to ac subgrid[15].

2) Comparison of Impact of dc droop gain on dc subgrid and HMS

The eigen value analysis for two scenarios like DCS1 and HMS is considered. The trajectory of dominant low frequency eigen values are presented in Fig. 9. The variation of droop gain of dc subgrid is increased from $2.5e-6$ pu to 0.021 pu. Similar to the previous case, it is observed that the HMS is stable for wide range of ac droop gain value in comparison to dc subgrid.

3) Effect of bidirectional power flow in HMS

To investigate the impact of power flow from dc to ac subgrid on the stability, each ac load distributed in ACS1 is considered to be 1.4 pu as shown in Fig. 3. The loci of the dominant low frequency modes for fixed m_{dc} and m_{ac} are depicted in Fig. 10(a) and (b) respectively, and m_{ic} is varied from $2.5e-6$ pu to 0.021 pu. To obtain this wide range of m_{ic} , the m_{ac} in (16) is varied when m_{dc} is

0.0207pu. The results in Fig. 10(a) show that m_{ic} has a significant effect on the damping factor and frequency oscillations. The low frequency modes which are close to the imaginary axis move towards the unstable region when $m_{ic} > 0.019 pu$. Though the reduce in IC droop gain improves the damping of the system, the small value of IC droop gain reduces the power flow from dc subgrid to ac subgrid.

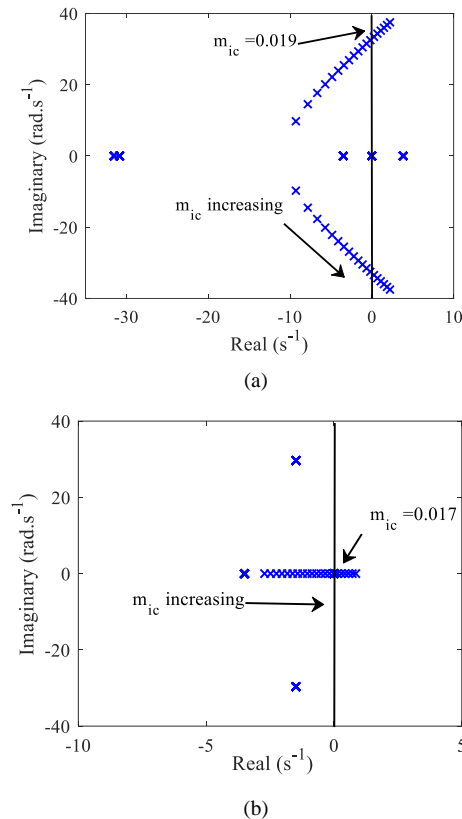


Fig. 10: The dominant low-frequency modes to change in droop coefficient of IC1 during power flow direction from dc to ac subgrid. (a) when $m_{dc}=0.0207pu$. (b) when $m_{ac}=0.017 pu$.

The results in Fig 10(b) shows when m_{dc} is varied and m_{ac} is chosen to be 0.017pu. The eigen value locations of ICs moves to right half plane and indicate the instability, and allowable range of droop gain of IC is decreased to 0.017 pu in compare to the previous condition.

Next, the results are shown to evaluate the stability margin under power flow direction from ac to dc subgrid, where dc load distributed in DCS1 is adopted to 1.4 pu.

Fig. 12 shows the impact of droop gain of IC (m_{ic1}). To investigate how the m_{dc1} can affect the system stability during this condition, the trace of the dominant low frequency modes for two conditions, when the $m_{dc} = 0.021pu$ and $m_{dc} = 0.016pu$ are compared. Similar to change in m_{ac} as shown in Fig. 7,

the low-frequency modes move towards right hand side, and the presence of poles on left hand plane in Fig. 10 indicates that the system is stable. The stability margin of m_{ic} is found to be 0.02 pu and 0.031 pu when m_{dc} is equal to 0.021 pu and 0.016 pu respectively. It can be seen that the effective damping of the HMS is increased when the droop gain of dc subgrid is decreased.

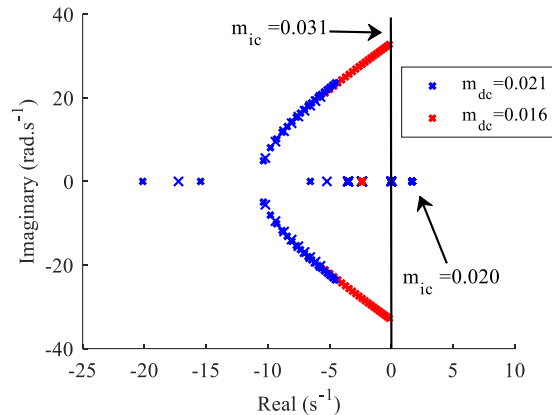


Fig. 11: The dominant low-frequency modes to change in droop coefficient of IC1 during power flow direction from ac to dc subgrid and droop gain of dc sub grid is fixed.

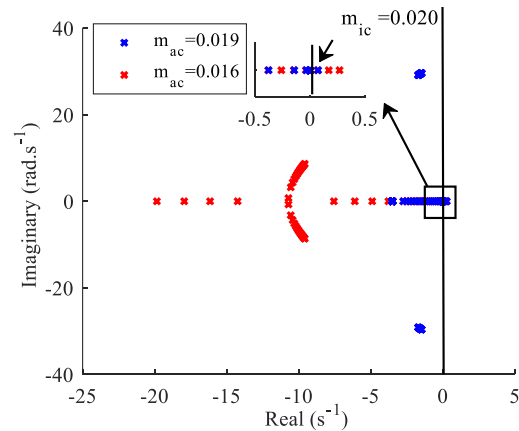


Fig. 12: Trace of dominant low frequency modes to change in droop coefficient of IC1 during power flow direction from ac to dc subgrid and droop gain of ac subgrid is fixed.

In the next case, selected two droop gain values of ac subgrid are 0.016 pu and 0.019 pu. The above mentioned procedure is followed to vary m_{ic} from $2.5e-6$ pu to 0.021 pu. It can be seen that the low-frequency modes move towards right hand side and reaches to unstable region when $m_{ic} > 0.02 pu$. By comparing the root locus of dominant low frequency modes of two ac droop gain values (0.016 pu and 0.019 pu), it can be noticed that the stability margin is independent of ac droop gain for power flow direction from ac to dc subgrid.

5. Conclusion

The issue of the small-signal stability of HIMSs formed by subgrid clusters is presented. Initially, the operation of droop-controlled ICs is investigated and the effects of IC droop gain settings on system stability among subgrids and locus of eigen values are plotted. It is found the pole move further outside the negative real plane for increasing power flow from DCS to ACS. Extensive scenarios are presented to demonstrate the system stability under the HIS control strategy with respect to different droop gain constants. The type of loading condition, cable impedance and filters for each subgrids are considered. Further, it is found that the instability in hybrid islanded microgrids can be mitigated with the integration of renewable integrated DC sources in DCS. Taking into account the nature of subgrids, the control loops are devised and analyzed, in which the power sharing between the ACS and DCS is presented.

References

- [1] K. Kurohane, T. Senjyu, A. Yona, N. Urasaki, T. Goya, and T. Funabashi, "A Hybrid Smart AC/DC Power System," *IEEE Trans. Smart Grid*, vol. 1, no. 2, pp. 199–204, Sep. 2010.
- [2] J. M. Guerrero, J. C. Vasquez, J. Matas, L. G. de Vicuna, and M. Castilla, "Hierarchical Control of Droop-Controlled AC and DC Microgrids—A General Approach Toward Standardization," *IEEE Trans. Ind. Electron.*, vol. 58, no. 1, pp. 158–172, Jan. 2011.
- [3] Y. Han, H. Li, P. Shen, E. A. A. Coelho, and J. M. Guerrero, "Review of Active and Reactive Power Sharing Strategies in Hierarchical Controlled Microgrids," *IEEE Trans. Power Electron.*, vol. 32, no. 3, pp. 2427–2451, 2017.
- [4] Y. Li and Y. W. Li, "Power Management of Inverter Interfaced Autonomous Microgrid Based on Virtual Frequency-Voltage Frame," *IEEE Trans. Smart Grid*, vol. 2, no. 1, pp. 30–40, Mar. 2011.
- [5] Y. A. R. I. Mohamed and E. F. El-Saadany, "Adaptive decentralized droop controller to preserve power sharing stability of paralleled inverters in distributed generation microgrids," *IEEE Trans. Power Electron.*, vol. 23, no. 6, pp. 2806–2816, 2008.
- [6] H. Liang, B. J. Choi, W. Zhuang, and X. Shen, "Stability enhancement of decentralized inverter control through wireless communications in microgrids," *IEEE Trans. Smart Grid*, vol. 4, no. 1, pp. 321–331, 2013.
- [7] L. Xiaonan et al., "Hierarchical Control of Parallel AC-DC Converter Interfaces for Hybrid Microgrids," *Smart Grid, IEEE Trans.*, vol. 5, no. 2, pp. 683–692, 2014.
- [8] P. C. Loh, S. Member, D. Li, Y. K. Chai, and F. Blaabjerg, "Hybrid AC – DC Microgrids With Energy Storages and Progressive Energy Flow Tuning," vol. 28, no. 4, pp. 1533–1543, 2013.
- [9] P. C. Loh, D. Li, Y. K. Chai, and F. Blaabjerg, "Autonomous operation of hybrid microgrid with ac and dc subgrids," *IEEE Trans. Power Electron.*, vol. 28, no. 5, pp. 2214–2223, 2013.

- [10] F. Blaabjerg, P. C. Loh, D. Li, and Y. K. Chai, "Autonomous operation of ac-dc microgrids with minimised interlinking energy flow," *IET Power Electron.*, vol. 6, no. 8, pp. 1650–1657, 2013.
- [11] A. A. A. Radwan and Y. A.-R. I. Mohamed, "Networked Control and Power Management of AC/DC Hybrid Microgrids," *IEEE Syst. J.*, pp. 1–12, 2014.
- [12] M. Amin and M. Molinas, "Small-Signal Stability Assessment of Power Electronics based Power Systems: A Discussion of Impedance- and Eigenvalue-based Methods," *IEEE Trans. Ind. Appl.*, pp. 1–1, 2017.
- [13] I. P. NIKOLAKAKOS, H. H. Zeineldin, M. S. El Moursi, and J. L. Kirtley, "Reduced-Order Model for Inter-Inverter Oscillations in Islanded Droop-Controlled Microgrids," *IEEE Trans. Smart Grid*, pp. 1–1, 2017.
- [14] I. P. Nikolakakos, H. H. Zeineldin, M. S. El-Moursi, and N. D. Hatziargyriou, "Stability Evaluation of Interconnected Multi-Inverter Microgrids Through Critical Clusters," *IEEE Trans. Power Syst.*, vol. 31, no. 4, pp. 3060–3072, 2016.
- [15] X. Li et al., "A Unified Control for the DC-AC Interlinking Converters in Hybrid AC/DC Microgrids," *IEEE Trans. Smart Grid*, pp. 1–1, 2017.
- [16] "IEEE Guide for Conducting Distribution Impact Studies for Distributed Resource Interconnection," *IEEE Std 1547.7-2013*, pp. 1–137, Feb. 2014.
- [17] N. Pogaku, M. Prodanović, and T. C. Green, "Modeling, analysis and testing of autonomous operation of an inverter-based microgrid," *IEEE Trans. Power Electron.*, vol. 22, no. 2, pp. 613–625, 2007.
- [18] A. A. A. Radwan and Y. A.-R. I. Mohamed, "Assessment and Mitigation of Interaction Dynamics in Hybrid AC/DC Distribution Generation Systems," *IEEE Trans. Smart Grid*, vol. 3, no. 3, pp. 1382–1393, Sep. 2012.